Earth and Planetary Science Letters 459 (2017) 394–405

Contents lists available at ScienceDirect

Earth and Planetary Science Letters

www.elsevier.com/locate/epsl

Wave speed structure of the eastern North American margin

B. Savage [a,*], B.M. Covellone [b], Y. Shen [b]

[a] Department of Geosciences, University of Rhode Island, United States
[b] Graduate School of Oceanography, University of Rhode Island, United States

ARTICLE INFO

Article history:
Received 26 July 2016
Received in revised form 15 November 2016
Accepted 17 November 2016
Available online 12 December 2016
Editor: P. Shearer

Keywords:
tomography
ambient noise
North America
craton

ABSTRACT

The eastern North American margin (ENAM) is the result of nearly a billion years of continental collision and rifting. To the west of this margin lies thick continental lithosphere of the North American craton, and to the east is oceanic lithosphere in the Atlantic. The substantial changes in lithosphere thickness at this boundary are thought to drive asthenosphere upwelling along the edge of the continent. Through iterative, full-waveform, ambient noise tomography, we observe a heterogeneous low wave speed margin along the continent in the upper mantle. Multiple low wave speed features imaged within the margin are consistent with asthenospeheric upwelling due to edge-driven convection. Also within the margin are high wave speed anomalies that maybe the remnants of eclogitic delamination of the Appalachian crustal root, which contribute to convection at the margin. Edge driven, small-scale convection keeps the margin weak and thus controls the large scale plate tectonic patterns and the crustal deformation. The imaged mantle wave speed anomalies, interpreted as edge-driven convection, correlate with and may increase the likelihood of damaging earthquakes in the eastern portion of North America.

1. Introduction

The eastern North American margin (ENAM) is presently a passive continental margin and the result of multiple episodes of continental collision and rifting dating back more than a billion years ago (Hoffman, 1988, 1991; Thomas, 2006). Thomas (2006) describes two complete Wilson cycles, the closing and opening of ocean basins associated with the assembly and breakup of supercontinents, that have shaped the ENAM. The first Wilson cycle that assembled Rodinia, the Grenville Orogen, and its subsequent breakup created the Iapetus Ocean between 1.35 and 0.53 Ga (Thomas, 2006). A second Wilson cycle began with the closing of the Iapetus Ocean and assembly of Pangea from the successive Taconic, Acadian and Alleghanian Orogenies, commonly referred to as the Appalachian–Ouachita Orogen, between 495 and 270 million years ago (Ma) (Thomas, 2006). Early Jurassic northeast striking rift structures place the break-up of Pangaea at approximately 230 Ma in present day southeastern North America (Schlische, 2003).

The initial rifting and breakup of Pangea and formation of the Atlantic basin are associated with multiple magmatic provinces scattered on both margins of the present day Atlantic basin. Two in particular, the Central Atlantic Magmatic Province (CAMP) and the East Coast Margin igneous province (ECMIP), Fig. 1, have been suggested as a result of either 1) a mantle plume or 2) continental rifting in the form of 2a) reactivation of Paleozoic structures or 2b) upwelling convection cells at the edges of cratons (White et al., 1987; White and McKenzie, 1989; Holbrook and Kelemen, 1993; Oyarzun et al., 1997; Wilson, 1997; McHone, 2000; Janney and Castillo, 2001; Puffer, 2003; Nomade et al., 2007; Beutel, 2009; King and Anderson, 1998).

A complex history of collision and breakup recorded on the continent and thick post rifting sediments along the Atlantic margin make unraveling the broad scale features in the lithosphere difficult through either direct sampling of material or active source seismology. Moreover, the resolution of previous wave speed models for North America vary widely across the continent and are primarily long wavelength, greater than 5°. Regardless, interpretations of the current state and origins of the ENAM have been made from various continental (van der Lee and Nolet, 1997; Goes and van der Lee, 2002; Godey et al., 2003; van der Lee and Frederiksen, 2005) and regional (Li et al., 2002, 2003; Rychert et al., 2005, 2007; Liang and Langston, 2009; Parker et al., 2013) scale seismic studies. The current station distribution of seismic networks deployed throughout the United States, as well as stations located in northeastern Canada and throughout the Caribbean, provide an extensive and dense coverage for ambient noise tomography of the ENAM to vastly improve the resolution of wave speed structures of the ENAM in a single wave speed model.

High resolution seismic images of lower crustal and shallow mantle structure beneath the ENAM can offer insight into the ex-

* Corresponding author.
E-mail addresses: savage@uri.edu (B. Savage), yshen@uri.edu (Y. Shen).

http://dx.doi.org/10.1016/j.epsl.2016.11.028
0012-821X/

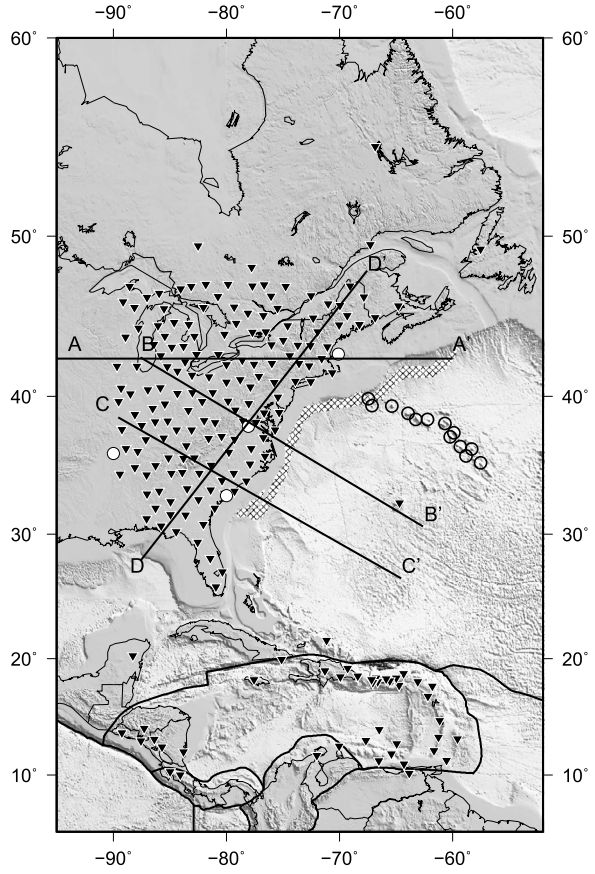

Fig. 1. 203 seismic stations, black inverted triangles, used for this study of the Eastern North American Margin (ENAM). Our entire computational domain is displayed within the map bounds. Modern plate boundaries are highlighted in thick black. The "New England Seamounts" are identified as black circles in the Atlantic and the East Coast Magnetic Anomaly, along the entire coast, and the Brunswick Anomaly, only in the south, are hatched. Cross section A through D are shown as straight black lines. Four white dots indicate significant earthquakes within the model.

tent of the rift related features. As the ENAM is mostly aseismic, ambient noise seismic data can provide high-quality measurements as the input data for tomographic models of the region. The surface waves measured with ambient noise methods employed here with periods >25 s are sensitive to crust and upper mantle Earth structure, key to the understanding of the relationship of tectonic provinces and the development of rifting.

The wave speed model presented here of the ENAM provides new and valuable insight of the upper 300 km, including the extent and depth of deformation of the lithosphere from rifting and plate tectonic forces. Taking advantage of the early stages of EarthScope's Transportable Array (TA) of seismic stations in the eastern United States, our model provides much higher resolved features than previous continent scale models.

2. Methodology

To determine the 3-dimensional (3D) seismic wave speed structure beneath the ENAM we use an iterative, finite-frequency tomography approach using full-waveform ambient noise seismic data. Empirical Green's functions are derived from continuously recorded broadband seismic data at periods up to 200 s. Use of empirical Green's functions (EGF) from ambient noise exploits up to 20+ years of broadband seismic data recorded at stations throughout North and Central America and the Caribbean, not reliant on earthquake distributions or earthquake source mechanisms. For stations within the Transportable Array (TA), we utilized as much continuous data as possible, around two years. Data from ambient noise reduces a source of error, from an earthquake's location and source mechanism, and is able to exploit temporary seismic station deployments that are unable to gather sufficient earthquake data during their deployments. Sources generating ambient noise are thought to occur from an interaction between the ocean, atmosphere and the sea floor (Ardhuin et al., 2015; Rhie and Romanowicz, 2004).

The methodology follows from Gao and Shen (2014) and Covellone et al. (2015). Continuous, vertical component seismic data recorded between 1990 and 2014 was gathered from IRIS DMC for 203 stations located in the eastern United States, Caribbean, Central and South America, Fig. 1. To extract usable Rayleigh wave signals from the raw data, an ambient noise processing procedure outlined in Shen et al. (2012) and Gao and Shen (2014) was used. After removing the instrument response a frequency time normalization (FTN) (Shen et al., 2012) was used to normalize the data. Using FTN is essential as it results in an increased signal to noise ratio and usable signals >100 s. Earthquake signals are removed by zeroing the amplitude during windows when earthquake signals are expected at a station and a cross correlation between station pairs is calculated with one station acting as the "virtual" source, s_i, and the other as the receiver, r_i. The cross correlated records are stacked and following a time derivative, represent our EGFs. Examples of the EGFs can be found in Supplemental Section S.1.

Synthetic seismograms are calculated by propagating seismic waves from a virtual source, vertical single force, to all receivers using a nonstaggered-grid finite-difference method (Zhang et al., 2012). The initial model is a combination of the global surface wave diffraction model, CUB (Ritzwoller et al., 2002), and AK135 (Kennett et al., 1995) at depths greater than 396 km.

EGFs and synthetics are filtered using a two-pass butterworth filter at five overlapping finite period bands 200–100 s, 150–75 s, 100–50 s, 75–30 s, 50–25 s, denoted as T_j, for $j = 1 \rightarrow 5$. Phase delays, dt, were measured between the data and synthetics by cross-correlation, following (Dahlen et al., 2000), for each frequency band. The methodology is termed "full-waveform" as the data, here empirical Green's functions, are directly compared to synthetic responses from a 3D Earth model. Low quality signals are removed from the measurement using a minimum signal-to-noise ratio, a minimum cross correlation coefficient criteria, see Supplemental Table S.1 and a minimum inter-station distance of $\Delta_{min} = c_{max} T_j$ where c_{max} was set to 4 km/s and T_j is the maximum period within a frequency band; see Luo et al. (2015) for inter-station distance limitations. Iteration 1, ite01, measured 17,624 station pairs, n, resulting in 53,186 total measurements. There are approximately equal number of measurements in each frequency band. The scattering-integral (SI) approach (Zhao et al., 2005; Zhang et al., 2007; Chen et al., 2007b, 2007a; Zhang and Shen, 2008) is used to construct strain green tensors (SGTs) and calculate finite-frequency sensitivity kernels $K_{\alpha,\beta}(s_i \rightarrow r_i, T_j, \mathbf{x}_k)$ between the source, s_i, and the receiver, r_i, for $i = 1 \rightarrow n$, within the period range of interest, T_j. The frequency-dependent phase delay, dt_{ij}, measurements and sensitivity kernels are used to invert for perturbations in α and β following

$$dt_{ij} = \iiint_{\oplus} \left[K_\alpha(s_i \rightarrow r_i, T_j, \mathbf{x}_k) d\alpha + K_\beta(s_i \rightarrow r_i, T_j, \mathbf{x}_k) d\beta \right] d\mathbf{x}^3$$

where the sensitivity kernels, K_α and K_β, are defined as in Zhao et al. (2005). Inversions were conducted at a variety of smoothing and damping values and the preferred model was chosen to minimize model norm and data misfit, see Supplemental S.2. The perturbations are then added to the 3D reference model at the end of each iteration. Following Covellone et al. (2015), density is